Results in Engineering 26 (2025) 105041

Contents lists available at ScienceDirect

Results in Engineering

journal homepage: www.sciencedirect.com/journal/results-in-engineering

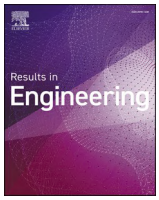

Research paper

Experimental study of solar thermal energy storage finned tanks filled with different storage materials (PCM, gravel, and water)

Waleed Khalaf Jabbar [a,b,*], Ahmed Kadhim Alshara [c], Asiem Sahib Allawy [b]

[a] Engineering Technical College in Misan, Southern Technical University, Iraq
[b] Engineering Technical College in Baghdad, Middle Technical University, Iraq
[c] College of Engineering, University of Misan, Al Amarah, Misan 62001, Iraq

ARTICLE INFO

Keywords:
Energy storage
Fins
Phase change material
Solar water heating
Thermal tanks

ABSTRACT

Thermal energy storage systems are vital to overcome the mismatch between the solar energy harvesting and demand employing several sensible and latent heat storage materials. This work experimentally evaluates the thermal performance of thermal energy storage tanks filled with gravel, phase change material (PCM), and water. Each tank was provided with 29 circumferential fins, and blanketed with a thermal insulation to minimize heat losses. The average temperature variation during heat charging and discharging and the energy stored for each tank was discussed and evaluated to specify the best storage medium. Findings indicated that the PCM tank displayed the best performance, exhibiting lowest heat loss rates during energy discharging, with values of 6.184, 6.505, 5.998, 8.221, and 9.388 W during peak 5 h. Meanwhile, the water tank showed heat losses of 8.599, 8.866, 9.121, 9.400, and 9.295 while, the gravel tank disclosed 9.496, 9.535, 9.802, 12.364, and 9.914 W, indicating poorer thermal performance. Study outcomes revealed that the PCM tank stored higher thermal energy compared with the other tanks, reaching a maximum of 0.87 kWh. Besides, the water tank stored 0.37 kWh thermal energy due to its high thermal capacity, while the gravel tank stored as lowest energy as 0.1 kWh. Equivalently, the PCM tank has stored 135 % and 770 % more energy than the water and gravel tanks, respectively. In conclusion, the PCM tank maintained higher temperatures and energy storage for a longer duration than other tanks, demonstrating high potential of PCM as an effective energy storage option.

1. Introduction

1.1. Background and importance of thermal energy storage

With the increasing demand for sustainable energy solutions, thermal energy storage (TES) systems have received a lot of attention for their capacity to improve energy efficiency and reduce variations in renewable energy sources, especially solar energy in hot locations [1]. TES plays an important role in optimizing energy usage in residential and industrial applications by storing excess thermal energy and releasing it as needed. Among TES technologies, Latent Heat Thermal Energy Storage Systems (LHTESs) using Phase Change Materials (PCMs) have emerged as a potential alternative due to their high energy storage density and temperature stability during phase transitions[2–4]. However, despite their benefits, most PCMs have low thermal conductivity, which severely limits heat transfer rates and prevents large-scale deployment [5–7].

To address this constraint, researchers have investigated a variety of augmentation strategies to speed heat transfer in PCM-based TES systems, including the incorporation of metal foams to improve thermal conductivity [8]. Using expanded fins to improve heat exchange efficiency [9]. Nanoparticle incorporation increases effective thermal conductivity [10,11]. Innovative heat exchanger designs improve heat extraction and use [12,13].

Recent studies have concentrated on enhancing PCM thermal performance through structural and material improvements. For instance, Yang et al. [8] developed a new TES unit with a shell-and-tube system by integrating porous metal foam into the gaps between the fins. Compared to the smooth tube, the unit reduced the melting/solidification time by up to 95.83 % and increased the average heat flux and Nusselt number by over 1800 % and 4700 %, respectively, at specific flow rates. Righetti et al. [14] explored a new engineering design by adding a metal structure to improve the thermal conductivity of the PCM. Three structures of different sizes, along with different heat fluxes, were used, embedded within a 3D aluminum frame. The PCM RT-70 made of paraffin wax was

* Correspondence author.
E-mail address: waleed.allamy@stu.edu.iq (W.K. Jabbar).

https://doi.org/10.1016/j.rineng.2025.105041
Received 13 February 2025; Received in revised form 5 April 2025; Accepted 21 April 2025
Available online 22 April 2025

Nomenclature

Abbreviations

PCM	Phase change material
LHTESs	Latent Heat Thermal Energy Storage Systems
HTF	Heat transfer fluid
TES	thermal energy storage

Symbols

m_p	Mass of PCM (kg).
m_w	Mass of water (kg).
m_g	Mass of gravel (kg).
$c_{p,g}$	Specific heat capacity of gravel (J/kg. K).
$c_{p,w}$	Specific heat capacity of water (J/kg. K).
$E_{s,solid}$	Sensible Heat of PCM (Heat of solid medium)
E_{latent}	Latent Heat of PCM
$E_{s,liquid}$	Sensible Heat of PCM (Heat of liquid medium)
$\dot{m}$	Mass flow rate (kg s^{-1})
Δh_m	Latent heat of fusion (J/kg)
v	Velocity (m s^{-1})
k	Thermal conductivity (W/m K)
T_m	Ambient temperature, K
T_i	Initial temperature, K
T_f	final temperature, K
F_m	melting fraction of PCM

Greek symbols

ρ	Density (kg/m^3)

Subscripts

I	Initial
f	Final
m	melting Absorbed
abs	Absorbed
L	Liquid
S	solid

used and compared to an empty reference box, where the 10 mm diameter structure proved to be the most efficient, reducing the charging and discharging times by up to 17 % and 26 %, respectively. Ying et al. [15] conducted a numerical simulation to design a TES unit using metal foam placed at the top and bottom in varying proportions as shown in Fig. 1. The heat transfer characteristics during melting were studied. The simulation showed that the flow of paraffin in the upper section was lower than that in the lower section by a volume ratio of 2:1 within the filling, making natural convection more effective in enhancing heat transfer. However, the top filling improved the thermal storage capacity more effectively. The results confirmed that a metal foam filling height of 0.75 led to a 7.47 % improvement in thermal storage efficiency. Guo et al. [16] investigated the impact of metallic fins and foam on enhancing heat transfer and improving thermal storage. The study showed that the hybrid structure, combining fins and metallic foam, outperformed all other configurations, achieving a melting time reduction of 83.35 % compared to a tube without fins. Khan et al. [17] explored various fin orientations to enhance the thermal performance of a TES system, with fatty acid used as a PCM. The inner tube was made of copper, and the casing was made of steel. The study revealed that in the case of the Y-shaped fin, the melting rate and energy accumulation increased. The TES capacity of the system improves by 10 % with Y-fins. A 7.6 % increase in the temperature of the heat transfer fluid increases the melting rate by 80 %. Zhang et al. [9] investigated phase change processes in LHTESs utilizing vertically mounted double-helical fins, horizontally oriented quadruple fins, and traditional fins as a reference. Their findings revealed that the first two configurations reduced the total melting time by 31 % compared to traditional fins. Additionally, they observed that flow velocity significantly influenced the charging process, with the flow direction opposing gravity yielding a more uniform thermal field. Liu et al. [18] investigated the heat transfer using a double helical heat pipe and employing palmitic acid as a thermal storage material, with different flow rates applied. The results showed a significant increase in the solidification process with higher flow rates. However, the change in the melting rate was minimal. During the PCM melting and solidification process, the temperature increase rate in the sidewall region is 34 % and 24 % greater than in the central region, respectively. Shen et al. [19] investigated the number of tubes used to enhance thermal performance efficiency in shell-and-tube TES tanks. They have found that tanks with a higher number of tubes reduced charging and discharging times by 50 % compared to tanks with fewer tubes. Additionally, increasing the fluid temperature to 70–80 °C

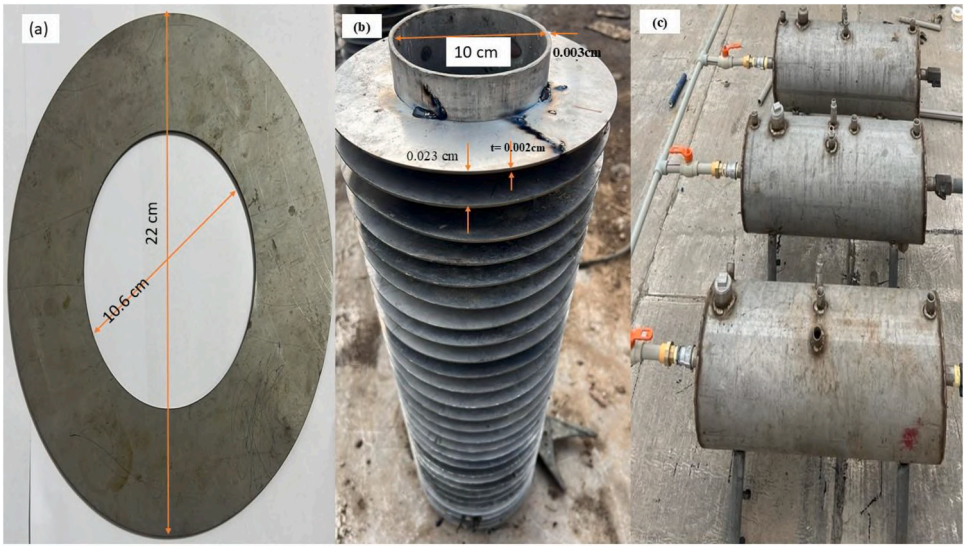

Fig. 1. (a) ring fins, (b) ring fins welded on the inner tube, (c) experimental tanks.

resulted in a 41 % reduction in charging time. Parsa et al. [20] conducted a study on the impact of the external shell shape on TES by three configurations: vertical-cylindrical, horizontal-cylindrical, and spherical, with identical shell volumes. The Paraffin wax was used as the PCM. The results indicated that the horizontal cylindrical shell reduced melting time by 32 %, while the vertical cylindrical shell achieved a 13 % reduction in melting time. The horizontal cylindrical shell demonstrated the best heat transfer rates, with an improvement of 41 %, whereas the vertical cylindrical shell exhibited a 12 % lower heat transfer rate. NematpourKeshteli et al. [21] performed a numerical simulation of a TES system utilizing a tri-lobed heat exchanger integrated with PCM. Their study explored performance improvements by incorporating lobed surfaces, Y-shaped fins, multi-walled carbon nanotubes (MWCNTs), and metal foam, either individually or in combination. The simulations, conducted using the finite volume method under varying operating conditions, aimed to enhance the inherently low thermal performance of PCMs in thermal storage applications. The findings revealed that increasing the modified Stefan number led to a 50.88 % reduction in melting time. Additionally, the inclusion of lobes and fins shortened the total melting duration by approximately 30.54 % compared to straight tubes. This reduction was further amplified to 74.26 % when lobes were combined with both nanoparticles and metal foam, and to 73.60 % when using metal foam alone. Pagkalos et al. [22]. verified and evaluated of materials used for TES systems-based water and paraffin were used as storage materials during two charging and discharging processes. Two tubes of different lengths were used, and a constant temperature was maintained during the analysis. The storage medium's volume was equal during the experiment, and the storage capacity of PCM exceeded that of water by approximately 4.1 times additional energy than water for the same storage tank volume. Elarem et al. [11] modified the design of a solar collector with an evacuated tube and PCMs by adding copper particles and fins showed significant results. The study indicated that the addition of fins and 1 % copper to the PCM greatly enhances heat transfer. Furthermore, the flow rate plays a crucial role in the melting of the PCM, with a flow rate of 0.003 kg s^{-1} being particularly effective. Jayaprakash et al. [23] designed an innovative TES system that using PCM to harvest and store solar energy at various temperatures. Erythritol and xylitol were chosen as key PCMs because of their melting qualities and compatibility with specified thermal criteria. To boost heat transfer efficiency, these materials were encapsulated in stainless steel, copper, and brass, with annular fins added for thermal performance. The system's efficiency was determined by analyzing the charging and discharging procedures, as well as the energy storage and release rates. Among the investigated configurations, encapsulation with stainless steel and annular fins was the most cost-effective option. Nassar et al. [24] used hybrid nanoparticles in copper foams to increase the thermal conductivity of PCMs. The impacts of metallic foams' specific surface area, weight ratio, and hybrid nanoparticles' weight fraction on the thermal characteristics of PCMs were studied. The results showed that PCM composites have much better thermal performance than pure PCM. In addition, increasing the weight fraction of metallic foams and hybrid nanoparticles resulted in a 37.7 % increase in thermal conductivity for the same copper. The researchers also discovered that adding more metallic foams and hybrid nanoparticles enhances heat conductivity. Furthermore, a particular surface area of 1600 m^2/m^3 has better thermal characteristics than other specific surface area values. Wang et al. [25] Investigated the effect of fluctuating inlet temperature on LHTES performance by combining experiments and simulations. Four intake temperature profiles were examined: stable, unsteady sinusoidal, unsteady cosine, and split (with two distinct states). The findings revealed that the unsteady sinusoidal inlet temperature reduced melting time by 5.3 % compared to the steady state and by 10.0 % compared to the cosine condition. These discoveries help to advance the development of phase-change TES devices, which promote the efficient use of renewable energy. Zhao et al. [26] numerically examined the influence of five different inlet temperature conditions on the melting behavior of PCMs in a conical spiral shell-tube energy storage system using Fluent, with experimental validation ensuring model accuracy. The study found that unsteady inlet temperatures reduce thermal stratification in the PCM. Compared to the steady-state heat source (T0), the melting time increased by 12.64 % and 10.11 % for heat sources TA and Ta, respectively, leading to a 4.98 % and 4.25 % rise in energy storage capacity while decreasing the average storage rate by 6.80 % and 5.32 %. Conversely, heat sources TB and Tb shortened the melting time by 18.20 % and 14.92 %, reduced the energy storage capacity by 4.54 %, and increased the average storage rate by 16.71 % and 12.19 %. These findings offer practical guidance for enhancing the thermal performance of energy storage systems. Siyabi et al. [27] experimentally evaluated the increase in TES using a multi-PCM approach. They investigated the behavior of multiple PCM configurations in different arrangements, with PCM melting temperatures ranging from 27 °C to 42 °C in both low and high arrangements and suitable melting times. The experimental results showed that the multi-PCM arrangement achieved a higher average temperature compared to low and high concentration material arrangements. The numerical analysis also addressed the impact of changing radial and axial storage dimensions, where the results showed that longer PCM storage enhances melting efficiency compared to wider storage for the same amount of PCM. Li et al. [28] presented an analysis to improve the performance of a LHTES system using twisted tube fins within a PCM enclosure. Both vertical and horizontal orientations were studied using the Finite Volume Method, and the Enthalpy-Porosity method was used to simulate the melting process. Different fin configurations were analyzed, including single, double, triple, and quadruple fins, along with the effect of penetrating the fin inside the tube. Paraffin wax was used as the PCM. The results showed that the triple fin in the vertical orientation and the double fin in the horizontal orientation significantly enhanced the melting process, reducing melting time by 11.2 % and 10.7 %, respectively, compared to the worst fin configuration, with improvements of 37.4 % and 30.5 % compared to the base case. Tiari et al. 2021 [29] conducted numerical investigations to study the effect of annular fins on the performance of a LHTES system during the charging and discharging processes. The system consists of a cylindrical container filled with RT55 as the phase change material, with a central pipe carrying the heat transfer fluid. The system was simulated using ANSYS Fluent 17.0. The fins were tested in two categories: ten fins with a thickness of 1.587 mm and twenty fins with a thickness of 0.794 mm. These fins were categorized into fixed and variable lengths, as displayed in Fig. 2. The best charging performance was achieved with twenty variable-length fins, resulting in a 73.7 % reduction in charging time. For discharging, twenty fins with a uniform length reduced the discharging time by 79.2 %. Overall, the twenty uniform-length fin configurations proved to be the most effective, reducing both charging and discharging times by 76.3 %. The fins also improved the thermal energy transfer to the phase change material, enhancing the system's performance.

1.2. Research gaps and limitations in previous studies

Despite substantial study on PCM thermal storage advances, some critical gaps exist in the literature. For instance, there were no direct comparison between PCM, gravel, and water under equivalent experimental settings. Moreover, there is limited research on long-term discharging efficiency, particularly for solar TES applications. Besides, few experimental setups were performed to utilize finned-tank configurations to test different storage materials, as well as a limited investigation of PCM performance with circumferential fin designs in a real-world solar heating system. In addition, most earlier studies concentrated solely on PCM improvements or novel heat exchanger designs, with no systematic assessment of how alternative thermal storage materials perform in the same configuration.

Fig. 2. Experimental thermal storage tanks and their accessories.

1.3. Study objectives

This study attempts to solve the following research gaps:

1- Examining the thermal performance of several TES materials (specifically PCM, gravel, and water) in a conventional finned-tank system coupled to a solar thermal heater.
2- Determining the charging and discharging processes of each storage medium under identical testing conditions.
3- Specifying the most effective TES material concerning the heat transfer rate and stored energy over time during charging and discharging processes.

This paper presents a thorough experimental analysis that will aid in the design optimization of TES systems for practical applications in renewable energy storage systems.

2. Materials and methods

2.1. Experimental set-up

To evaluate the characteristics of a novel system for generating sensible and latent heat energy, an experimental setup was designed and constructed at the Technical Engineering College of Misan, Iraq (31.8379°N, 47.1421°E). The proposed system comprises three primary tanks, a water pump, a solar-powered heater, and a data logger, as illustrated in Figs. 1 and 2. The solar heater consists of evacuated glass tubes designed to heat water to high temperatures resulting incident solar radiation during the day. This heated water is then supplied to TES tanks containing both sensible and latent storage materials. To minimize heat loss, 5 cm thick fiberglass insulation blanket, having thermal conductivity of 0.043 W/m·K [30], has covered the three tanks, and 8 cm thick thermal foam insulation was used along the heater. A pump is used to facilitate water flow through the tanks to store heat transferred by the hot water in the thermal storage materials, which are placed between the core and the shell. The solar heater is made of iron galvanized material. The water pump and a flow rate meter were employed to maintain a controlled flow of the heat transfer fluid throughout the system.

A recycled solar water heater was structured as a sustainable and clean energy source, associated to three experimental tanks (Fig. 2). This design aims to enhance TES while addressing challenges such as leakage and the limited thermal conductivity of PCMs. Three thermal tanks were manufactured from stainless steel tube type 304, with details presented in Table 1. The tank consists of an inner tube with a diameter of 10 cm and a length of 70 cm and 29 fins mounted on the outer circumference of the inner tube with a thickness of 2 mm, which helps to improve and accelerate the melting process by 80 %[31], which were created using a CNC laser cutting machine for high accuracy, as shown in Fig 0.1. The fins are surrounded by a casing. An outer casing with a diameter of 28 cm and the same length. The hot water coming from the solar heater passes through the inner tube, and the amount of water entering and exiting can be controlled by valves installed at the inlets and outlets of each tank. To maximize heat storage, the thickness of the inner and outer tubes of the three thermal tanks is 0.3 cm. The outer casing is fully insulated with 5 cm thick glass wool to reduce heat loss. Each tank has an inlet and outlet for the flow of the heat transfer fluid (water). In addition, each tank has a 5 cm diameter opening at the top for charging the heat storage materials and another at the bottom for discharging. The tanks also have five openings for connecting temperature measuring devices and monitoring the changes during charging and discharging through a multi-channel temperature reader.

Table 1
Design specifications of TES tanks.

Specifications	Value
Thermal storage tank dimensions (Diameter × length)	28 × 70 cm
Inner tube (Diameter × length)	10 × 70 cm
Tube thickness	0.3 cm
Inlet and exit water pipe diameter	3.81 cm
Number of fins	29
Dimeter of ports for charging and discharging	5 cm
Slots to connect thermal sensors	5
Fins pitch	0.0023 cm
Fin height ∅	22cm

The tanks were filled with various thermal storage materials, including water, gravel, and PCM. its heat is supplied to the tanks through an evacuated tube solar heater that has been manufactured and installed in a location under direct sunlight, with water acting as the heat transfer medium. The solar heater is connected to the three tanks and employs valves to control the amount of water entering. Water flows at a consistent rate of one liter per hour via a 10-cm-diameter inner tube. A flow meter and control valve are put at the end of each tank to regulate the flow rate during the draining operation.

2.2. Experimental procedure of research

The following stages describe the experimental methods utilized in the research.

1. The thermal tank is supplied with water from the solar heater, and the hot water flows into the inner tube of the tank.
2. Heat exchange takes place between the water in the core and the saving materials in shell, ensuring that the PCM are heat treated. Fins are attached to the outer perimeter of the inner tube, which helps to increase the heat transfer by conduction.
3. The water coming out of the tanks is recycled into the solar heater, which increases the water temperature and accelerates the flow of hot water at the inlet
4. The water pump adjusts the water flow rate to prevent any pressure buildup within the tank.
5. A flow meter is connected at the inlet of the tanks to calculate the flow amount when charging, and three flow meters are connected at the outlet of each tank to calculate the flow when discharging, in order to determine the amount of latent heat LHS, which depends on the heat gain and loss in the storage materials.
6. A multi-channel data logger is connected to the tank to monitor the inlet, exit, and thermal tank temperatures. Five thermocouples were linked to each solar thermal tank to precisely monitor its temperature.
7. A weather observation system collects and records important environmental data such as wind speed, radiation from the sun, humidity, and the outside temperature.
8. The amount of heat stored also depends on the rate of temperature change, the volume of the phase change material, and the type of material inside the tank.
9. The experiments were conducted from 22 to 26 June 2024, with readings taken every 15 min during the charging process, then the discharging process begins until the temperature of the outgoing water reaches normal.

2.3. TES materials equipped into the tanks

There are two main types of latent heat storage: storing heat by increasing the temperature of a material without causing a phase change (such as water or gravel). Latent heat storage, using PCMs, such as paraffin wax to store and release energy during a phase transition (melting-solidification process).

2.3.1. Water as a TES material

Water is a popular material for TES systems due to its high specific heat capacity, availability, and low cost. It is generally used in systems intended to store sensible heat, in which energy is stored by raising the temperature of the water.

2.3.2. Paraffin wax rubitherm RT-50 as a TES material

Paraffin wax is a popular PCM because of its high latent heat capacity, consistent performance, availability and safety characteristics. Paraffin can absorb a lot of thermal energy during melting and release it during solidification, making it perfect for applications that require consistent temperature regulation. However, paraffin wax has a low thermal conductivity, which might impede heat transfer. To solve this, improvements to the TESs design are required to optimize heat transfer. The paraffin used (shown in Fig. 3), with the trade name Rubitherm RT50 (PCM), was obtained from a German company, and its thermal properties are listed in Table 2 as reported by the source.

2.3.3. Gravel as a TES material

Gravel is a common material consisting of small rock fragments. In thermal storage applications, gravel is often used as a means of storing and releasing thermal energy. This is achieved through a process called sensible heat storage, where the gravel absorbs and retains heat as its temperature increases and releases it when its temperature decreases. Gravel has a good thermal conductivity, allowing it to absorb heat and distribute it efficiently throughout the storage medium. Gravel is a relatively inexpensive material compared to other thermal storage media, making it an economical choice for large-scale storage systems. The gravel was obtained from the Al-Tayeb area in Maysan, with particle sizes ranging from 1 cm to 2 cm to minimize the effect of size on its use in the geometric configuration (Fig. 4). Table 2 summarizes the thermal and physical characteristics of the materials studied.

The integration of a recycled thermal storage materials in this study significantly enhances the sustainability of TES applications by minimizing material waste, improving energy efficiency, and reducing environmental impact. By utilizing locally sourced and recyclable materials, including water, gravel, and stainless steel, the proposed system supports both economic and environmental sustainability. Future research could further investigate the life cycle assessment and carbon footprint analysis to provide a more comprehensive evaluation of the long-term benefits of recycled TES designs.

2.4. Measurement devices

Temperature measurements at various positions within the TES tank

Table 2
Thermal properties of TES materials.

Properties	Units	Rubitherm RT-50	Gravel	Water
Melting Temperature, Tm	°C	46–51	–	–
Latent Heat of Fusion	J/kg	160,000 ± 7.5 %	–	–
Specific Heat, c_p	J/kg. K	2000 Solid 2200 Liquid	840	4179
Thermal Conductivity, k	W/m · K	0.2	1.5	0.613
Density, ρ	kg/m^3	880 solidus 770 liquidus	1.6	997.1
Volume Expansion	%	12.5	–	–

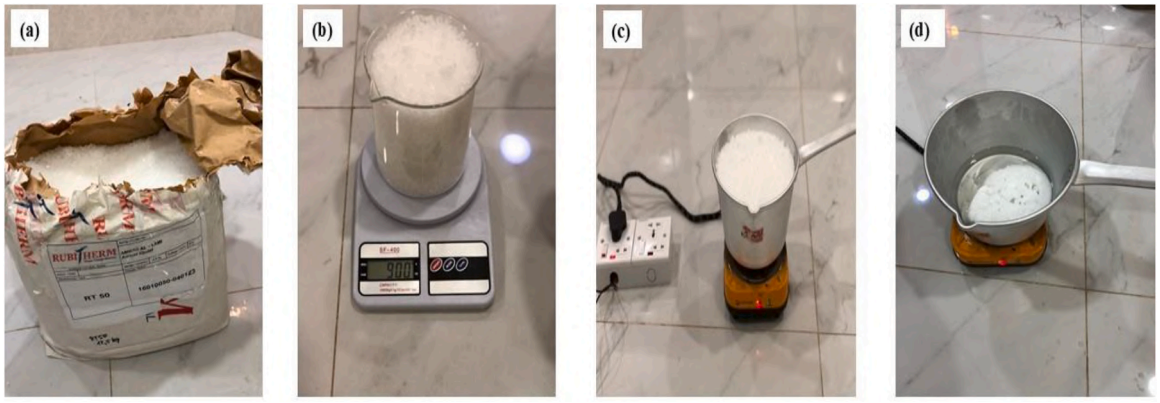

Fig. 3. PCM preparation: (a) Rubitherm RT50, (b) weighting of PCM, (C) heating of PCM using electrical heater, (d) liquid PCM.

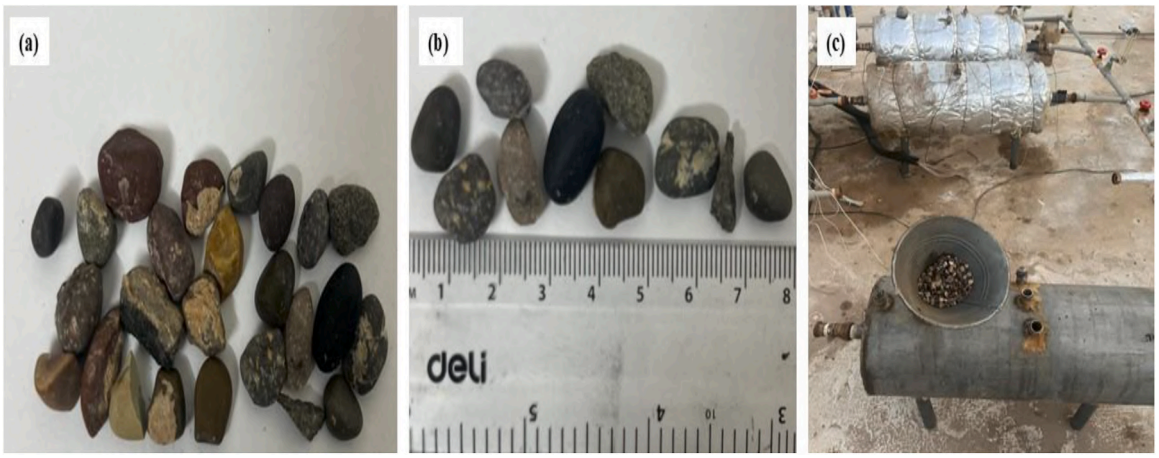

Fig. 4. (a) Gravel TES, (b) gravel dimensions, (c) insertion of gravel into the tank.

were conducted using five K type thermocouples per tank, along with two additional thermocouples for the inlet and outlet ports. All thermocouples were calibrated using the central organization for standardization and quality control (COSQC), as detailed in Table 3. These measurement devices were connected to a 16-channel datalogger (MDCS Multichannel datalogger), configured to record temperature readings at 15-minute interval throughout the experiment. The datalogger was equipped with a synchronization interface, allowing for real-time data transfer directly to the computer. The hot spots on the solar collector were measured using infrared thermometer to perceive the thermocouples. The HTF (water) was circulated using an efficient water pump with a constant mass flow rate (0.28 kg s^{-1}). The mass flow rate was graduated using a precise flowmeter having accuracy of 1 %. Fig. 5 presents a multi-channel data logger that records temperature readings at 15-minute intervals throughout the charging and discharging processes. The (Madincos MPD580 - MPD580), a 16-channel device from Xiamen Madincos Automation Co., Ltd., captures the transient temperature distribution of the material at different locations during the process charge and discharge, as illustrated in Table 3. The data loggers were calibrated at COSQC.

The CURCONSA Wi-Fi Weather Station is a cutting-edge piece of meteorological equipment that allows for exact monitoring of indoor and outdoor environmental conditions. It has an 8-inch color LCD display that shows real-time meteorological data such as temperature, humidity, wind speed, wind direction, precipitation, air pressure, sun radiation, and UV index. Additionally, the technology provides weather forecasting capabilities based on acquired atmospheric characteristics, as shown in Fig. 5. The system is fueled by several sources. Indoor Console: Works with a 5 V adaptor (included) or three AAA batteries (not provided) as backup. Outdoor Sensor Array: Powered by three AA batteries (not included), the integrated solar panel acts as an extra energy source, ensuring continuous data transmission.

2.5. Specifications of the solar collector and solar heater

The solar tank has a storage capacity of 120 liters and is paired with a solar collector consisting of 16 evacuated glass tubes. Each collector tube measures 175 cm in length, while the solar collector itself has a width of 110 cm. The height of the solar tank from the base of the collector is 100 cm, with a 5 cm gap between each tube. The maximum operating pressure for the solar water heater, equipped with an evacuated tube solar collector, is 0.5 kg/cm^2. The solar collector, a key component of the system, is constructed from evacuated borosilicate glass tubes. Each tube consists of two concentric glass layers, with the inner tube's outer surface coated with a specialized solar-selective layer designed to absorb and convert solar radiation efficiently into heat. The space between the inner and outer glass tubes is evacuated and permanently sealed, creating a vacuum that acts as a highly effective insulator.

Table 3
Measurement device specifications as calibrated by the manufacturer.

Measurement device	Mode	Serial NO	Error (°C)
Temperature Reader with TC (K)	MPD580–16-C1-N.	20,201,221,004	−1.7
Digital thermometer	PL-120-T1	180,513,418	0.4

2.6. Energy analysis

2.6.1. Thermal energy absorbed by water (E_w)

To compare the three TES tanks containing different thermal storage materials (gravel, PCM, and water), The amount of heat absorbed during the charging process of the three tanks was calculated, according to Eqs. (1) to (6) [32,33].

$$E_w = m.c_{p,w}(\Delta T). \quad (1)$$

Here, m: denotes the mass of the water, while $c_{p,w}$ represents its specific heat capacity of water about J/kg. K. T_f and T_i are the final and initial temperature.

2.6.2. Thermal energy absorbed by water and gravel (E_g)

The heat stored for substances such as water and gravel, which do not undergo phase changes, is determined using:

$$E_g = E_w + E_g \quad (2)$$

$$E_g = m_w.c_{p,w}.(\Delta T) + m_g.c_{p,g}.(\Delta T) \quad (3)$$

where is m_w is the mass of water (kg), m_g is the mass of gravel (kg), $c_{p,w}$ is the specific heat capacity of water (J/kg. K), $c_{p,g}$ is the specific heat capacity of gravel (J/kg·K), and ΔT is the temperature difference between the final and initial temperatures (i.e., $T_f - T_i$).

2.6.3. Thermal energy absorbed by PCM (E_p)

$$E_p = E_{s,solid} + E_{latent} + E_{s,liquid} \quad (4)$$

$$E_p = \int_{T_i}^{T_m} m\, c_p dT + mF_m\Delta h_m + \int_{T_m}^{T_f} mc_p dT \quad (5)$$

$$E_p = m_p\left[c_{p,s}(T_m - T_i) + F_m\Delta h_m + c_{p,l}(T_f - T_m)\right] \quad (6)$$

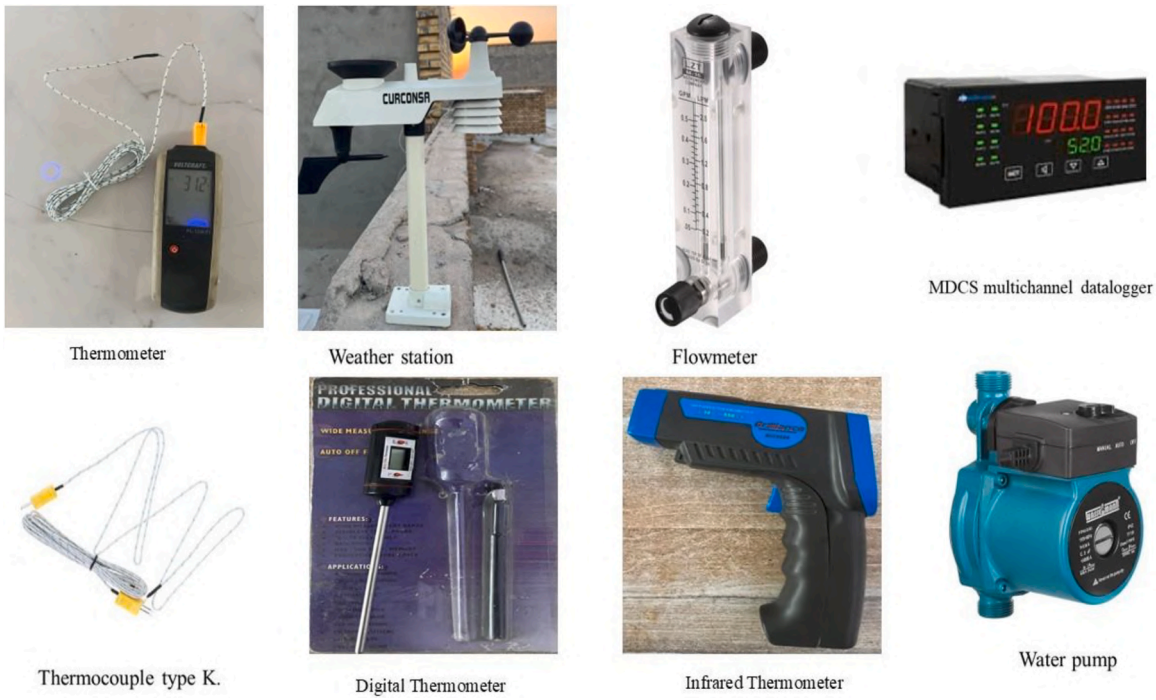

Fig. 5. Measurement devices.

Here, $m_p$is the mass of the PCM (kg), $c_{p,s}$ is the sensible heat of the solid medium, $c_{p,l}$ is the sensible heat of the liquid medium, F_m is the melting fraction of PCM, and Δh_m is the latent heat of fusion for the PCM (J/kg).

2.6.4. Average temperatures during the charging cycle

The thermal rate of each material can be estimated using the basic arithmetic equation for the (mean temperature. T_{avg}), which is given as follows:

$$T_{avg} = \frac{\sum T_i}{N} \tag{7}$$

where T_{avg} is the average temperature,T_i is the temperature at different points in time, and N is the number of recorded temperature values.

To assess the credibility of the experimental results, an uncertainty analysis was carried out using standard error propagation methods. Uncertainty occurs from measurement limits in sensors, data gathering systems, and environmental conditions. The overall uncertainty is determined using individual uncertainties from several measured parameters, according to Michael and Iniyan [34]. The uncertainty analysis was made to quantify the heat transfer rate for the HTF presented in Eq. (8).

$$\dot{Q} = \dot{m} \cdot c_p \ (T_{in} - T_{out}) \tag{8}$$

In which the heat transfer rate is dependent on the uncertainty of devices used to measure the mass flow rate and inlet and outlet temperatures (i.e., $\dot{Q} = f(\dot{m}, T_{in}, T_{out})$. Consequently, Eq. (9) suggested by Michael and Iniyan was reformulated as presented in Eq. (9):

$$\frac{U_{\dot{Q}}}{\dot{Q}} = \sqrt{\left(\frac{U_{\dot{m}}}{\dot{m}}\right)^2 + \left(\frac{U_{T_{in}}}{T_{in}}\right)^2 + \left(\frac{U_{T_{out}}}{T_{out}}\right)^2} \tag{9}$$

were U stands for the uncertainty of measured data by measurement tools. Accordingly, the calculated uncertainty was varied between 0.3 % and 0.4 %.

3. Results and discussion

In this work, we study the performance of the LHTS unit during charging and discharging, as demonstrated by the experimental model in Fig. 2. Three tank designs utilizing different storage materials, such as gravel, PCM, and water are compared in terms of several energy aspects. Engineering enhancements have been made to the tanks, focusing on design improvements and adding more fins while maintaining the same number 29 fins and type of manufacturing metal. To ensure consistency, the tanks are integrated into a uniform system, with identical boundary conditions applied across all experimental scenarios.

3.1. Study location conditions

The experimental work was conducted over five consecutive days in June, from the 22 to the 26, under the conditions of Maysan Governorate- Al Amarah City, in southern Iraq. This location is characterized as a dessert climate with a good potential for solar energy applications [35]. This month experienced a notable rise in temperature, with high ambient temperatures and solar radiation. All weather data, including wind speed, ambient temperature, and solar radiation, were recorded using the weather station (CURCONSR), as detailed in Table 4. The data were collected at 15-minute intervals throughout the experiment,

Table 4
Average weather and working conditions during experiments.

Days	Outlet collector's temperature (°C)	Ambient temperature (°C)	Wind speed (m s^{-1})	Solar radiation (W/m^2)
Day 1	72.6	41.8	3.2	874.8
Day2	73.3	42.2	2.1	917.6
Day 3	71.6	42.1	3.6	832.1
Day 4	75.4	42.1	2.5	932.9
Day 5	74.2	42.5	2.6	918.8

systematically tabulated, and stored on a computer. Data were recorded during the charging process, where the average ambient temperature reached a maximum of 42.12 °C. The average solar radiation during the experiment days was 895.252 W/m^2, and the average wind speed was 2.8 m s^{-1}.

3.2. Charging and discharging cycles

The charging cycle begins with preparing the tank and ensuring an adequate water supply. The tank is first filled with water, and valves 1 and 2 are opened while valve A remains closed (Fig. 6). Water is then supplied to the solar heater to capture the maximum temperature readings. Once the solar heater is ready, hot water flow is initiated by opening control valve 3, allowing heated water to enter the system. To maintain a consistent flow rate, control valve 4 is adjusted and monitored using a flow meter. For system operation, valves 5, 7, and 9 are opened, and the pump is activated to circulate the water through the system. Temperature data is collected using a data logger connected to 15 sensors strategically placed within the setup. The process also involves a recirculation phase where valves 6, 8, 10, 11, 12, 13, and 14 remain open. This setup ensures that any water lost during the cycle is returned to the solar heater, where it is replenished with hot water to maintain system efficiency. As shown in Fig 6, the time used to charge the cycle was four hours, starting from 10:00 a.m. to 12:00 pm. Data was recorded every 15 min through the data collector. The temperature of the water entering the solar collector was recorded as 27 °C, and the temperature leaving the solar heater was recorded as 67–68 °C (Table 4). The average outlet temperature of each storage tank is listed in Table 5. A mass flow meter was installed in the part that comes after control valve No. 4 to ensure distribution and control of the amount of water entering each tank. The hot water passes through valves 5, 7, and 9 to the inner pipe, which has a diameter of 10 cm.

As could be noted in Table 5, the outlet average temperature of the PCM tank is generally higher than that of gravel and water. This could be

Table 5
Average outlet temperature of storage tanks.

	$T_{average}$, gravel	$T_{average}$, PCM	$T_{average}$, water
Day 1	48.57	57.13	50.88
Day 2	48.99	56.82	50.72
Day 3	46.17	56.06	47.93
Day 4	43.49	54.21	51.16
Day 5	49.14	50.52	50.75

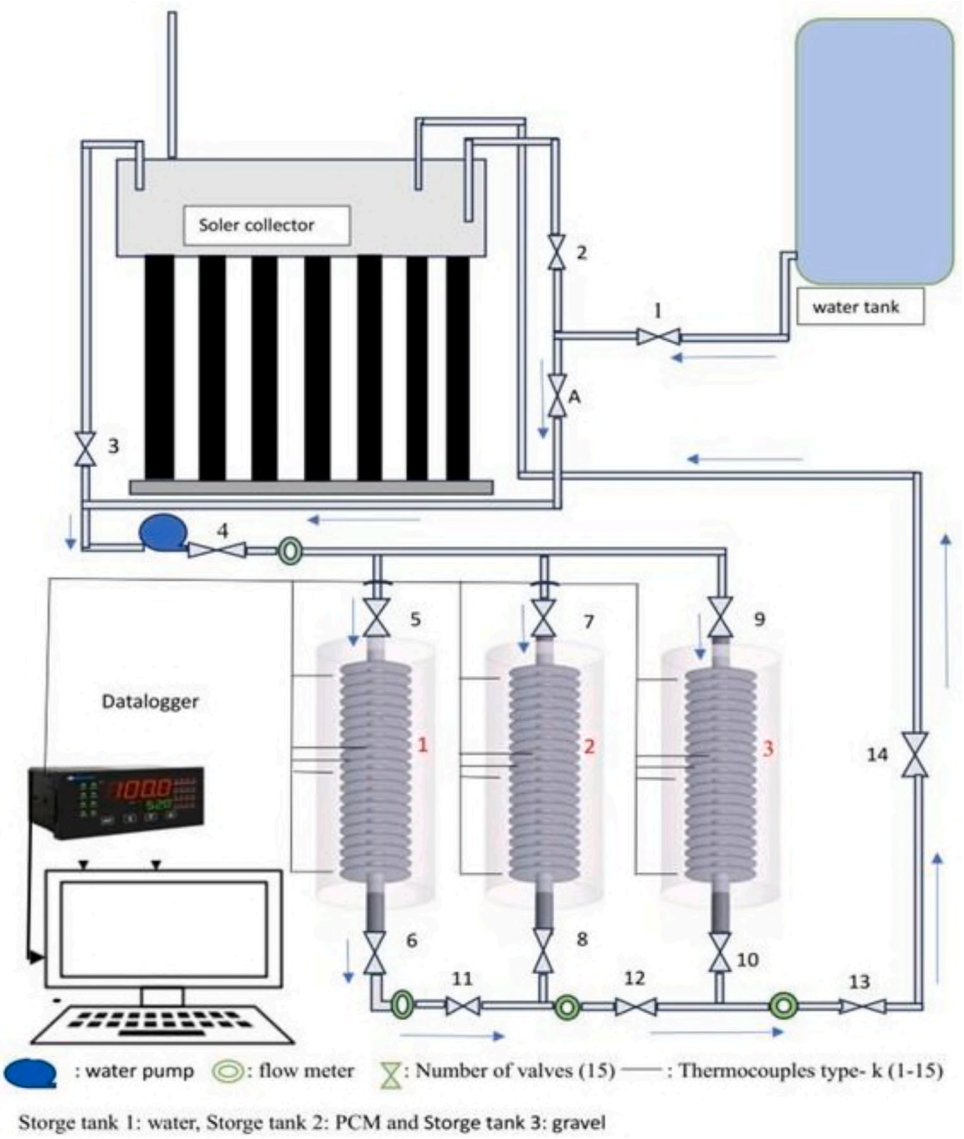

Fig. 6. Schematic of the experimental setup indicating the location of valves.

attributed to the high melting temperature of PCM (50 °C) which kept the outlet temperature of working temperature always in this limit. From the other hand, the outlet temperature of water tank was also higher than that of gravel thanks to the massive water quantity and specific heat. These values are suitable for domestic hot water usage in various applications, including buildings.

The discharging process in the thermal storage system, which consists of three modified tanks, starts by closing valves 2 and 3 and opening valve A to redirect water directly from the main tank to the three storage tanks (Fig. 6). A pump is activated to determine the water flow rate through the valves connected to the outlets of each tank, monitored using a flow meter.to prevent water from flowing back into the solar heater, valve 14 is closed. this action ensures the discharging process operates efficiently, closed the charging cycle. During the discharging phase, valves 8, 6, and 10 are opened to release water, with the discharged volume carefully monitored. Temperature and flow data are recorded throughout the process to track the system's performance accurately. The temperature is compared over time until each tank reaches thermal equilibrium. At this point, the respective tank is closed, Record data over time until the water temperature returns to ambient levels. The tank that has longest to discharge the most efficient, as it indicates amount of stored thermal energy.

3.3. Average temperatures during the charging cycle

Fig. 7 illustrates the average charging temperature versus time for day the three tanks at a flow rate of 1 L per hour. The storage materials were heated using water as a heat transfer fluid (internal heating method). The charging temperature varied over time due to intermittent solar radiation influenced by climatic conditions. The temperature changes over time, depicted in the figure, illustrate the effect of intermittent solar radiation and the characteristic thermal behaviors of each material. PCM showed relatively stable temperatures, consistent with phase change properties. Gravel, while less responsive to sudden temperature changes, showed consistent heat retention. In contrast, water, being highly reactive to external heating, showed the most significant fluctuations. This comparison underscores the advantages and limitations of each material: PCM is well suited for applications requiring temperature stabilization, gravel provides a cost-effective solution for heat storage, and water excels in scenarios that prioritize rapid heat absorption and transfer. The rise in water temperature on the fourth day may imply a high specific heat capacity, however the steep drop on the fourth day is most likely due to external cooling influences rather than the material's intrinsic qualities.

3.4. Average temperatures during charging and discharging cycle

Fig. 8 illustrates the average discharging temperature versus time for (day) the three tanks at a flow rate of 1 L per hour. The water acquires temperature from the different storage materials used in the tanks. The temperature during discharge fluctuates over time. In this scenario, the discharging process in the three tanks continues until the heat stored during the charging process is completely released, and the time for each tank is observed.

The discharge process in TESs emphasizes the efficiency of releasing stored energy, which is influenced by factors such as the discharge efficiency of the storage material and temperature distribution. Water exhibits strong performance during discharge due to its high thermal conductivity, enabling rapid heat transfer. However, it has a lower energy storage density compared to PCM.

Gravel, relying solely on sensible heat storage, delivers slower and less efficient discharge performance compared to water. In contrast, PCM excels in discharge efficiency due to its phase transition (from solid to liquid and vice versa), which facilitates the release of substantial latent heat at a relatively constant temperature. While enhancements like fins significantly improve PCM performance, the absence of such features can lead to delays in thermal energy release.

The temperature distribution is a critical factor in evaluating storage materials. PCM offers nearly constant temperatures during discharge, attributed to its latent heat, making it highly suitable for applications requiring thermal stability. Water provides a fast and efficient discharge rate but is prone to significant temperature drops during the process. Gravel and water are more cost-effective and easier to manage, but PCM remains the preferred choice for applications demanding high energy storage density and thermal stability.

Fig. 9 illustrates the average temperature distribution of gravel, PCM, and water with time (h) during charging and discharging on the first day. The charging process on the left demonstrates a steady rise in temperature for all materials due to heat absorption. PCM demonstrates the maintaining of a consistent rise due to its latent heat absorption during the phase change. Water exhibits a rapid temperature rise due to its high thermal conductivity, while gravel shows a slower increase, attributed to its lower heat transfer properties. On average, the temperature inside the water, gravel and PCM-filled tanks were 51.4 °C,

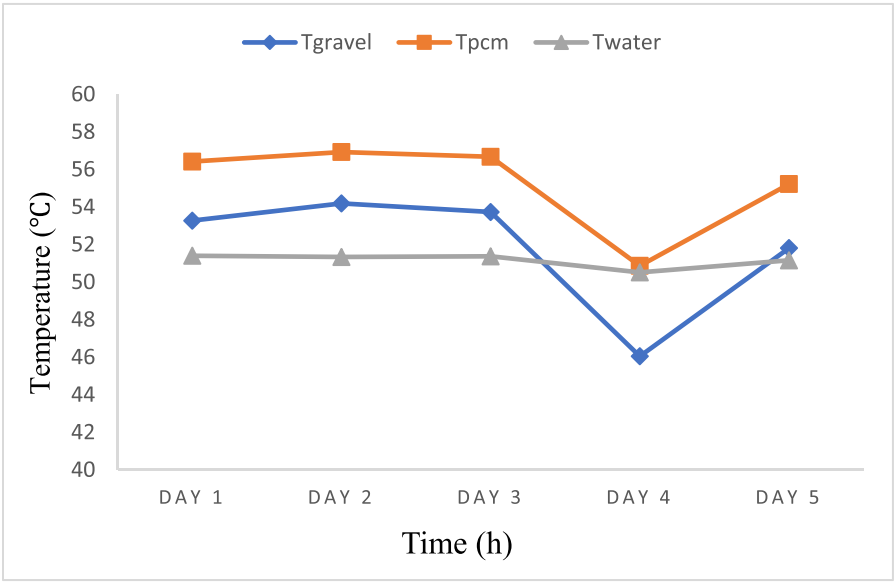

Fig. 7. Average temperatures in the system during the charging cycle over 5 days.

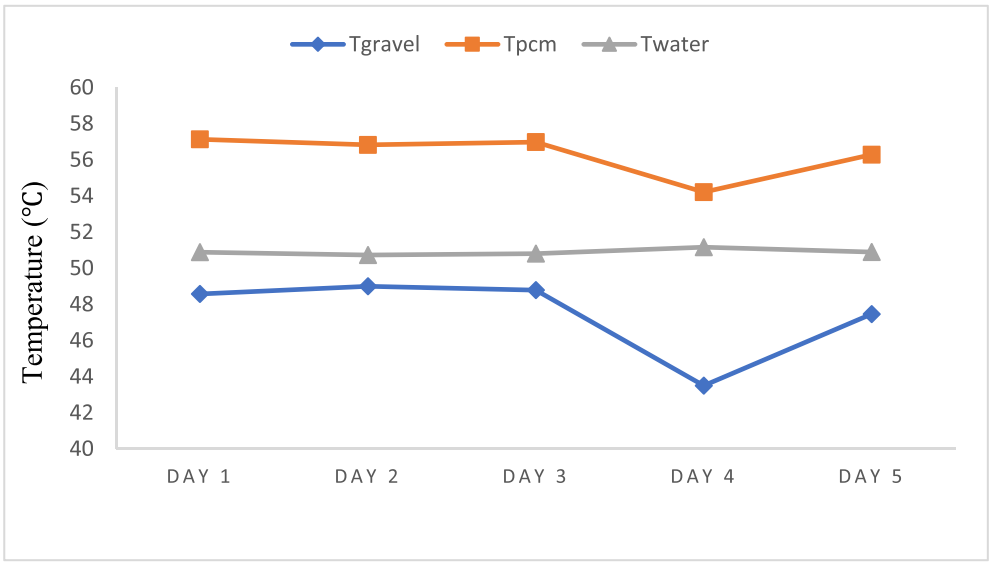

Fig. 8. Average temperatures in the system during the discharging cycle over 5 days.

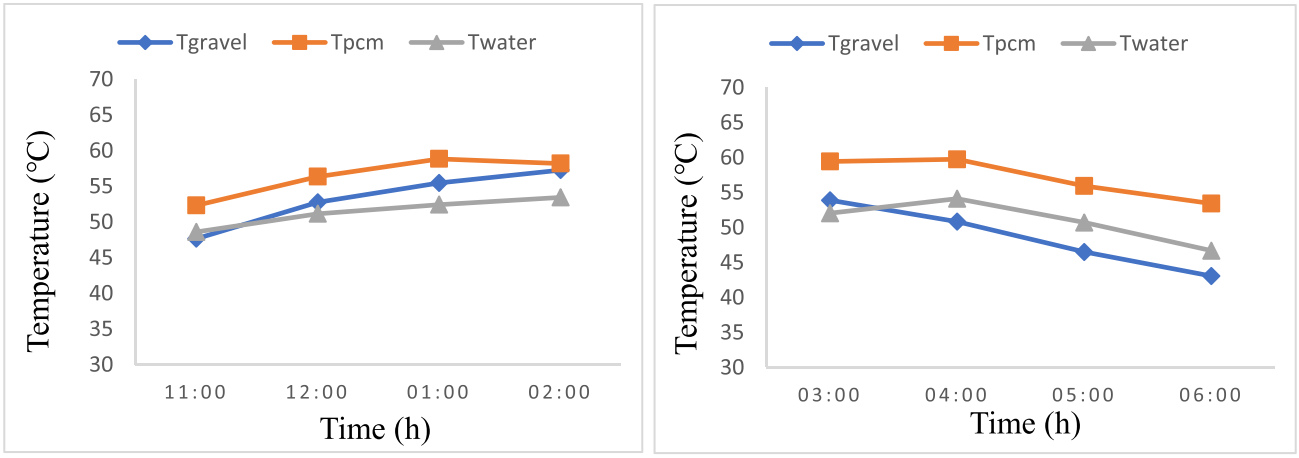

Fig. 9. Temperature profiles during charging (left) and discharging (right) on the first day.

53.3 °C and 56.4 °C, respectively during charging process. Whereas the average temperature of these tanks was respectively 50.9 °C, 48.6 °C and 57.1 °C, during discharging process.

On the right, the discharging process indicates a decrease in temperature as heat is released. PCM maintains a relatively high temperature over time, emphasizing its capacity to release latent heat at a nearly constant rate. Water cools down rapidly, reflecting its high heat transfer efficiency but limited thermal storage density. Gravel shows the slowest cooling rate, consistent with its reliance on sensible heat storage.

These temperature trends underline the distinct thermal behaviors of each material, highlighting PCM's superiority for applications requiring temperature stability, water's efficiency for rapid heat transfer, and gravel's cost-effectiveness despite its slower performance.

Fig. 10 depicts temperature during the charging (a) and discharging (b) processes from the second to the fifth day. The graphs show that the phase change material (PCM) maintains greater temperatures than other materials (gravel and water) during both charging and discharging phases, demonstrating its high thermal capacity and efficiency in heat storage.

During the charging process, the PCM temperature remains reasonably steady at a higher level, whereas other materials (gravel and water) respond more slowly to temperature increases. This shows that PCM can successfully absorb and store heat for an extended period of time. As the days pass, temperatures rise somewhat, presumably due to the cumulative effect of continual charging.

During the discharge phase, all materials experience a steady temperature reduction. However, PCM maintains greater temperatures for longer periods of time, proving its effectiveness in preventing heat loss over time. Gravel, on the other hand, has a faster temperature drop, indicating a larger discharge rate, due to its reduced thermal capacity when compared to PCM and water.

The comparison of the three materials' behavior over several days indicates a similar tendency, with small deviations that could be attributable to environmental changes or cumulative thermal impacts. These findings demonstrate the importance of using phase change materials in TES systems to improve thermal performance and long-term storage efficiency.

Initially, PCM shows a faster temperature rise than gravel and water, suggesting its effectiveness in heat absorption. After 1:00 PM, the temperature difference was gradually reduced, indicating that PCM is approaching thermal saturation and reaching an equilibrium phase. Water often responded slower but at a lower temperature than PCM and gravel, indicating a larger heat loss rate. In summary, it could be stated that paraffin wax is the most efficient material for long-term TES. It demonstrated superior and energy retention compared to water and gravel, which are more suitable for short-term applications due to their

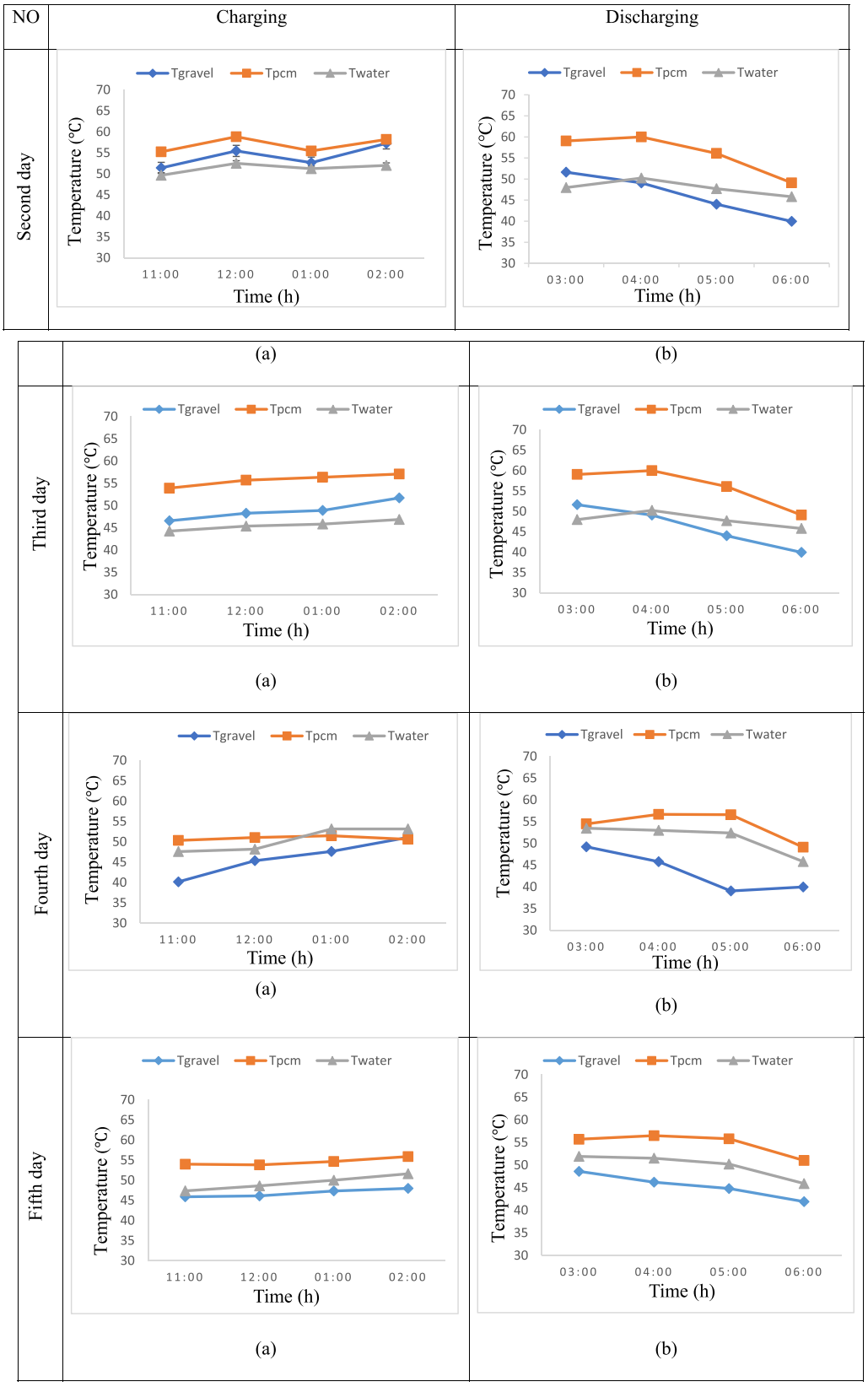

Fig. 10. Temperature profiles during charging (a) and discharging (b) in the 2nd, 3rd, 4th and 5th days.

significant performance decline over time. The tank containing water performs faster during the charging and discharging processes due to the high thermal conductivity of water, which allows for rapid heat transfer. However, this tank is not suitable for long-term heat storage due to the quick loss of heat to the surrounding environment. The tank containing gravel exhibits moderate performance, Paraffin wax (PCM) is the ideal choice for TES, especially in applications that require maintaining heat for extended periods. Paraffin wax has the highest efficiency in during

charging and discharging processes, making it ideal for applications that require long-term TES. Conclusively, fins helped improve the thermal performance by increasing the PCM thermal conductivity.

Fig. 11 shows that the gravel curve discharge rates on day 4, which means a rapid loss of stored energy. On the other days, the energy levels gained remain relatively high, indicating that the gravel is less efficient at conserving energy for long periods. PCMs exhibit the lowest energy gained compared to gravel and water over the time period, showing a gradual and steady increase over the five days without significant fluctuations. As for the performance of water, it is intermediate between gravel and PCMs, with relatively stable behavior in the initial days, followed by a noticeable increase on the fourth day and then a slight decrease on the fifth day, which is lower than on the fourth day. From the graph, it could be noticed that the best performance for TES materials is shown by the PCM, as they exhibit the lowest energy loss rates, meaning the stored energy remains for a longer time. On the other hand, gravel is the least efficient in retaining energy, as the graph shows a significant rise during the discharge process, indicating rapid energy loss. Meanwhile, the performance level of water is intermediate between gravel and paraffin (RT-50), making it an acceptable option but not as efficient as phase change materials.

3.5. Analysis of heat loss rate and stored energy

Fig. 12 shows the heat loss rate (in Watts) for each TES tank over five experimental days. The results showed that the PCM tank had the lowest heat loss rates during energy discharging process, with values of 6.184, 6.505, 5.998, 8.221, and 9.388 W in the first, second, third, fourth and fifth days, respectively. Correspondingly, the water tank had intermediate heat loss rates, recording 8.599, 8.866, 9.121, 9.400, and 9.295 W, while the gravel tank disclosed the highest heat loss rates of 9.496, 9.535, 9.802, 12.364, and 9.914 W. These results show that the gravel tank had the highest heat losses indicating poorer thermal performance compared to PCM and water tanks. The PCM tank had proved superior thermal storage capacities by reducing heat loss and achieving a more stable temperature profile over time. This resulted in a maximum TES of 0.87 kWh, which is 135 % and 770 % more than that of the water and gravel, respectively. Water, with its relatively large specific heat capacity, stored 0.37 kWh of energy, making it a better choice to gravel but less effective than PCM. Gravel had the poorest performance, storing only 0.1 kWh of thermal energy, owing to its lower thermal capacity and higher heat dissipation rates. Overall, the PCM tank performed better than the other storage media in terms of energy retention, making it the best option for TES applications.

Temperatures were recorded for the three different storage materials: gravel, PCM and water at certain time intervals during the thermal charging procedure. The statistics show that all three materials gradually grow in temperature, but at different rates, indicating the differences in thermal characteristics. Specifically, the average temperature of gravel tank was raised steadily from 45.5 °C to 59 °C by the end of the time period. However, in the PCM tank, the temperature was increased dramatically from 52.95 °C to 63.07 °C, showing a high thermal capacity, while the water tank showed a similar trend as the PCM tank, but with a slower rate, rising from 48.5 °C to 53.4 °C.

Over five consecutive days of observation, the maximum stored energy values calculated were 347, 3698.216, 3892.52, 3827.752, and 3946.34 kJ under the operating conditions outlined in Tables 4 and 5. The average rate of energy storage in the PCM tank was approximately 3.148 kW. Besides, gravel absorbs and retains heat as its temperature rises and releases it as the temperature drops since gravel is characterized by good thermal conductivity. According to Cascetta et al. [36]a particle diameter of 10 mm, with a consistent length-to-width ratio, was suggested as the optimal value for achieving the best thermal performance [37] demonstrating that particle size significantly impacts thermal performance [38]. The thermal properties of gravel have been well-characterized at high temperatures. The thermal storage tank containing gravel recorded energy values over five days of about 248.158, 314.764, 541.974, 311.541, and 533.917 kJ, respectively. Besides, the thermal energy stored by the water tank over the five days was 783.4882, 1570.0336, 1227.666, 1420.782, and 1818.0492 kJ. The thermal energy achieved in the PCM tank was the highest among the three tanks, reaching a maximum of 3147,852.6 J. The water tank was following with a high thermal capacity and stored energy reaching about 1364,006 J, while that stored into the gravel tank was the least, reaching 390,071 J.

Although limited literature studies were performed in this research area, the results presented in the current work are essential showing an additional contribution to the field. A summary of literature studies outcomes compared with those of the current work are listed in Table 6.

4. Conclusions

This study focused on three thermal energy storage tanks containing different storage materials: gravel, PCM, and water. The storage tanks

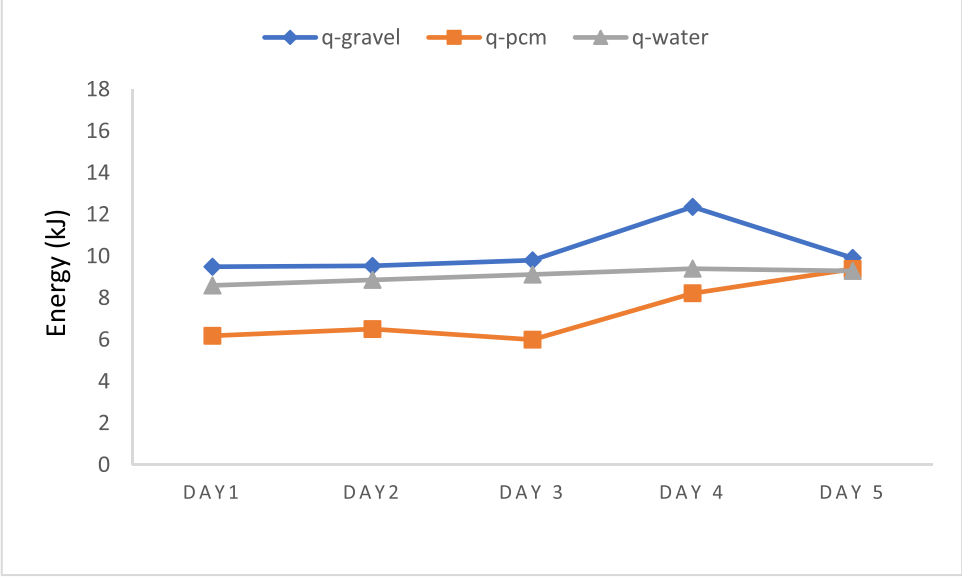

Fig. 11. Analysis of stored energy in different materials during discharging process.

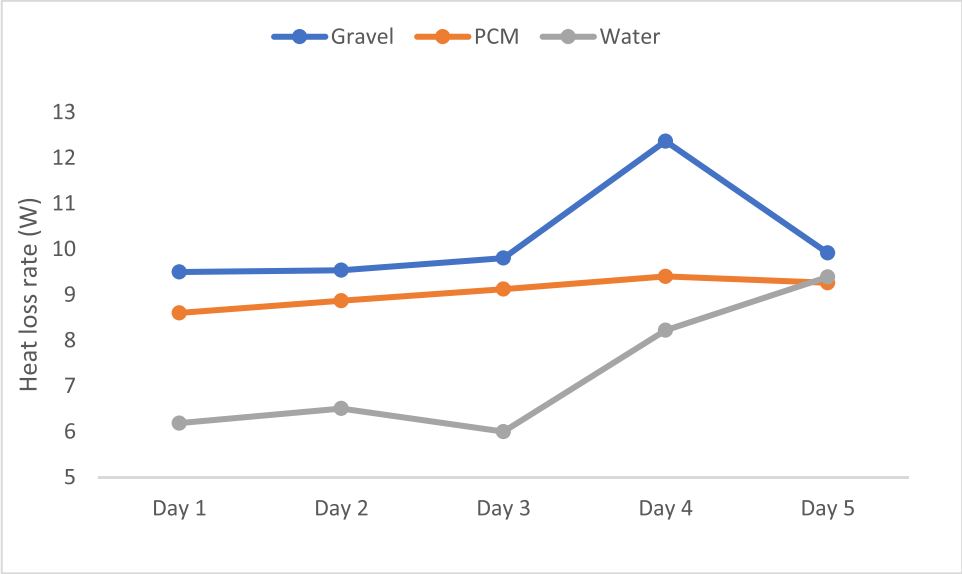

Fig. 12. Heat loss rate of TES systems over experimental days.

Table 6
Summary of the findings from studies published in previous literature, along with a comparison to the results of the current study.

Reference	PCM type	Modification	Key findings
Yang et al. [8]	Paraffin	Metal foam in a shell and tube system	charging/discharging time decreased by 95.83 %.
Righetti et al. [13]	RT-70 Paraffin	embedded 3D metal structure.	Charging/discharging time was lowered by 17 % and 26 %.
Guo et al. [14]	Paraffin	Hybrid fin-foam structure	Improved heat transfer; melting time reduced by 83.35 %.
Khan et al. [15]	Fatty acid PCM	Y-shaped fins	Enhanced melting rate and heat transfer.
Parsa et al. [18]	Paraffin	cylindrical/ spherical shell.	The horizontal shell improved heat transfer by 41 %.
Current Study	RT-50 Paraffin, Water, Gravel	29 circumferential fins in finned tanks	PCM tank achieved highest thermal energy (0.87 kWh), followed by water (0.37 kWh), and gravel (0.1 kWh)

were designed with a 10 cm diameter internal tube surrounded by 29 fins, enclosed within an outer shell with a diameter of 28 cm and a length of 70 cm. The compact design, combined with 29 fins, significantly enhanced thermal conductivity during the charging and discharging processes under a uniform flow of water as the heat transfer fluid. Higher temperatures were observed in the tank containing RT-50 PCM, followed by the tank containing water. This is attributed to the high thermal capacity of water. The melting and solidification processes of the PCM started in the region near the inner tube of the LHTES, followed by the region near the fins. Due to the effect of buoyancy, the last region to melt or solidify was the uppermost part. The thermal energy achieved in the PCM tank was the highest among the three tanks, reaching 0.87 kWh, while the water and gravel-based tanks stored energy of about 0.37 and 0.1 kWh, respectively. In other words, the PCM tank stored 135 % more energy than the water tank, and 770 % more energy than the gravel tank. The potential of PCM to store energy in latent form was superior. Compared to water and gravel, PCM has the largest capability for TES, as evidenced by the higher mean temperature over time. This demonstrates its effectiveness in absorbing and slowly releasing heat due to its phase change properties. Besides, the gravel had a moderate thermal performance compared to water and PCM, with temperatures higher than water but lower than PCM, indicating a medium thermal storage capacity. Therefore, the water has lowest heat storage capacity due to its fast heat transfer rate, leading it to quickly equilibrate with its surroundings.

Some suggestions for future work derived from the current research could be summarized as follows:

1. PCM has the finest heat storage performance, making it ideal for use in thermal energy storage systems, such as solar thermal and building heating. However, exploring the optimal operating range for PCMs still not specified.
2. Material costs should be considered, as PCM is normally more expensive than gravel and water, although this is offset by its high efficiency.
3. Using a combination of materials (such as PCM and gravel) could be an effective way to improve performance while lowering expenses.

CRediT authorship contribution statement

Waleed Khalaf Jabbar: Writing – original draft, Resources, Investigation, Formal analysis, Data curation, Conceptualization. **Ahmed Kadhim Alshara:** Writing – review & editing, Supervision, Investigation, Formal analysis, Conceptualization. **Asiem Sahib Allawy:** Writing – review & editing, Supervision, Formal analysis, Conceptualization.

Declaration of competing interest

The authors declare that they have no known competing financial interests or personal relationships that could have appeared to influence the work reported in this paper.

Data availability

Data will be made available on request.

References

[1] S. Mohammed Radhi, S. Al-Majidi, M. Abbod, H. Al-Raweshidy, Predicting solar power generation utilized in Iraq power grid using neural network, Misan J. Eng. Sci. 3 (2024) 38–62, https://doi.org/10.61263/mjes.v3i1.72.
[2] A. Aljehani, S.A.K. Razack, L. Nitsche, S. Al-Hallaj, Design and optimization of a hybrid air conditioning system with thermal energy storage using phase change

composite, Energy Convers. Manage 169 (2018) 404–418, https://doi.org/10.1016/j.enconman.2018.05.040.
[3] B.C. Zhao, R.Z. Wang, Perspectives for short-term thermal energy storage using salt hydrates for building heating, Energy 189 (2019) 116139, https://doi.org/10.1016/j.energy.2019.116139.
[4] Q. Al-Yasiri, A.K. Alshara, M. Al Sudani, A. Al Khafaji, M. Al-Bahadli, Advanced building envelope by integrating phase change material into a double-pane window at various orientations, Energy Build. 328 (2025) 115140, https://doi.org/10.1016/j.enbuild.2024.115140.
[5] Y. Liu, X. Li, Y. Xu, Y. Xie, T. Hu, P. Tao, Carbon-enhanced hydrated salt phase change materials for thermal management applications, Nanomaterials 14 (2024), https://doi.org/10.3390/nano14131077.
[6] N. Modi, X. Wang, M. Negnevitsky, Solar Hot water systems using latent heat thermal energy storage: perspectives and challenges, Energies. (Basel) (2023) 16, https://doi.org/10.3390/en16041969.
[7] B. Kanimozhi, B.R.R. Bapu, Experimental study of thermal energy storage in solar system using PCM, Adv. Mat. Res. 433–440 (2012) 1027–1032, https://doi.org/10.4028/www.scientific.net/AMR.433-440.1027.
[8] X. Yang, J. Yu, T. Xiao, Z. Hu, Y.L. He, Design and operating evaluation of a finned shell-and-tube thermal energy storage unit filled with metal foam, Appl. Energy 261 (2020) 114385, https://doi.org/10.1016/j.apenergy.2019.114385.
[9] S. Zhang, L. Pu, L. Xu, R. Liu, Y. Li, Melting performance analysis of phase change materials in different finned thermal energy storage, Appl. Therm. Eng. 176 (2020) 115425, https://doi.org/10.1016/j.applthermaleng.2020.115425.
[10] A.A. Eidan, A. Alsahlani, M.J. Alshukri, A.I. Alsabery, Experimental investigation of a solar evacuated tube collector embedded with a heat pipe using different nanofluids and controlled mechanical exciting pulsations, Int. J. Thermofluids 20 (2023) 100415, https://doi.org/10.1016/j.ijft.2023.100415.
[11] R. Elarem, T. Alqahtani, S. Mellouli, W. Aich, N. Ben Khedher, L. Kolsi, A. Jemni, Numerical study of an evacuated tube solar collector incorporating a Nano-PCM as a latent heat storage system, Case Stud. Thermal Eng. 24 (2021) 100859, https://doi.org/10.1016/j.csite.2021.100859.
[12] W. Lin, W. Zhang, Z. Ling, X. Fang, Z. Zhang, Experimental study of the thermal performance of a novel plate type heat exchanger with phase change material, Appl. Therm. Eng. 178 (2020) 115630, https://doi.org/10.1016/j.applthermaleng.2020.115630.
[13] H. Al-Lami, D.S.J. Al-Saedi, A.A.H. Almaidi, Q. Al-Yasiri, Conjoint effect of nanofluids and baffles on a heat exchanger thermal performance : numerical approach, Misan J. Eng. Sci. 3 (2024) 137–155, https://doi.org/10.61263/mjes.v3i2.105.
[14] G. Righetti, L. Doretti, C. Zilio, G.A. Longo, S. Mancin, Experimental investigation of phase change of medium/high temperature paraffin wax embedded in 3D periodic structure, Int. J. Thermofluids 5–6 (2020) 100035, https://doi.org/10.1016/j.ijft.2020.100035.
[15] Q. Ying, H. Wang, E. Lichtfouse, Numerical simulation on thermal behavior of partially filled metal foam composite phase change materials, Appl. Therm. Eng. 229 (2023) 120573, https://doi.org/10.1016/j.applthermaleng.2023.120573.
[16] J. Guo, Z. Liu, Z. Du, J. Yu, X. Yang, J. Yan, Effect of fin-metal foam structure on thermal energy storage: an experimental study, Renew. Energy 172 (2021) 57–70, https://doi.org/10.1016/j.renene.2021.03.018.
[17] L.A. Khan, M.M. Khan, Role of orientation of fins in performance enhancement of a latent thermal energy storage unit, Appl. Therm. Eng. 175 (2020) 115408, https://doi.org/10.1016/j.applthermaleng.2020.115408.
[18] Z. Liu, L. Zeng, M. Sheng, Y. Yan, W. Li, H. Su, Experimental and numerical research on thermal characteristics of phase change thermal storage device, Case Stud. Thermal Eng. 58 (2024) 104358, https://doi.org/10.1016/j.csite.2024.104358.
[19] G. Shen, X. Wang, J. Yu, Y. Bin, S. Zhong, S. Yang, J. Wang, Experimental investigation of thermal performance of vertical multitube cylindrical latent heat thermal energy storage systems, Environ. Sci. Pollut. Res. 31 (2024) 46447–46461, https://doi.org/10.1007/s11356-024-31864-7.
[20] N. Parsa, B. Kamkari, H. Abolghasemi, Enhancing thermal performance in shell-and-tube latent heat thermal energy storage units: an experimental and numerical study of shell geometry effects, Int. Commun. Heat Mass Transfer 154 (2024) 107398, https://doi.org/10.1016/j.icheatmasstransfer.2024.107398.
[21] A. NematpourKeshteli, M. Iasiello, G. Langella, N. Bianco, Optimization of the thermal performance of a lobed triplex-tube solar thermal storage system equipped with a phase change material, Heliyon. 10 (2024) e36105, https://doi.org/10.1016/j.heliyon.2024.e36105.
[22] C. Pagkalos, G. Dogkas, M.K. Koukou, J. Konstantaras, K. Lymperis, M. G. Vrachopoulos, Evaluation of water and paraffin PCM as storage media for use in thermal energy storage applications: a numerical approach, Int. J. Thermofluids 1–2 (2020) 100006, https://doi.org/10.1016/j.ijft.2019.100006.
[23] J. V, G. S, B. N, S.K. M, K.P. K, N. Kaliappan, Experimental investigation of cascaded thermal energy storage systems using finned encapsulated phase change materials, Results. Eng. 25 (2025) 104395, https://doi.org/10.1016/j.rineng.2025.104395.
[24] A. Nassar, E. Nassar, I. Rivilla, J. Labidi, A.G. Fernández, F. Sarasini, A.Abu El Fadl, M. Younis, Enhancing the thermal transfer properties of phase change material for thermal energy storage by impregnating hybrid nanoparticles within copper foams, Results. Eng. 21 (2024), https://doi.org/10.1016/j.rineng.2024.101885.
[25] Y. Wang, Q. Mao, Y. Zhao, Y. Tan, Experimental and numerical study of the melting process of phase change materials with novel finned heat storage tank under non-steady state conditions, Energy 320 (2025), https://doi.org/10.1016/j.energy.2025.135230.
[26] Y. Zhao, Q. Mao, Y. Zhang, Experimental and numerical analysis of cosine wave heat source on thermal storage performance of a conical spiral shell-tube energy storage system, Energy 306 (2024), https://doi.org/10.1016/j.energy.2024.132529.
[27] I. Al Siyabi, S. Khanna, T. Mallick, S. Sundaram, Experimental and numerical study on the effect of multiple phase change materials thermal energy storage system, n. d.
[28] J. Li, Z.R. Abdulghani, M.N. Alghamdi, K. Sharma, H. Niyas, H. Moria, A. Arsalanloo, Effect of twisted fins on the melting performance of PCM in a latent heat thermal energy storage system in vertical and horizontal orientations: energy and exergy analysis, Appl. Therm. Eng. 219 (2023), https://doi.org/10.1016/j.applthermaleng.2022.119489.
[29] S. Tiari, A. Hockins, M. Mahdavi, Numerical study of a latent heat thermal energy storage system enhanced by varying fin configurations, Case Stud. Thermal Eng. 25 (2021) 100999, https://doi.org/10.1016/j.csite.2021.100999.
[30] Q. Al-Yasiri, M. Szabó, Hourly analysis of temperature and heat gain reduction for building envelope-compacted phase change material in extremely hot conditions, J. Energy Storage 68 (2023) 107838, https://doi.org/10.1016/j.est.2023.107838.
[31] S.M. Borhani, M.J. Hosseini, A.A. Ranjbar, R. Bahrampoury, Investigation of phase change in a spiral-fin heat exchanger, Appl. Math Model. 67 (2019) 297–314, https://doi.org/10.1016/j.apm.2018.10.029.
[32] W.K.J. Allamy, I.A.H. Al-Najati, Residential space solar heating by thermally activating the space roof structure using evacuated tube solar collector in Iraq, J. Mech. Eng. Res. Develop. 44 (2021) 318–328.
[33] W.K.J. Allamy, I.A.H. Al-Najati, A thermal insulator manufacturing, using solid residuals from pulp and paper factories in Missan City, AIP. Conf. Proc. (2021) 2338, https://doi.org/10.1063/5.0067247.
[34] J.J. Michael, S. Iniyan, Performance analysis of a copper sheet laminated photovoltaic thermal collector using copper oxide – water nanofluid, Solar Energy 119 (2015) 439–451, https://doi.org/10.1016/j.solener.2015.06.028.
[35] H.A. Salim, J.R. Rashed, Techno - economic feasibility analysis of hybrid renewable energy system by using particle optimization technique for the rural border areas in Iraq : case study, Misan J. Eng. Sci. 3 (2024) 14–31, https://doi.org/10.61263/mjes.v3i2.83.
[36] M. Cascetta, G. Cau, P. Puddu, F. Serra, Numerical investigation of a packed bed thermal energy storage system with different heat transfer fluids, Energy Procedia 45 (2014) 598–607, https://doi.org/10.1016/j.egypro.2014.01.064.
[37] C. Xu, X. Li, Z. Wang, Y. He, F. Bai, Effects of solid particle properties on the thermal performance of a packed-bed molten-salt thermocline thermal storage system, Appl. Therm. Eng. 57 (2013) 69–80, https://doi.org/10.1016/j.applthermaleng.2013.03.052.
[38] G. Dalla Santa, F. Peron, A. Galgaro, M. Cultrera, D. Bertermann, J. Mueller, A. Bernardi, Laboratory measurements of gravel thermal conductivity: an update methodological approach, Energy Procedia 125 (2017), https://doi.org/10.1016/j.egypro.2017.08.287.